Pergamon

Cement and Concrete Research 33 (2003) 755–762

CEMENT AND CONCRETE RESEARCH

Behaviour of lightweight expanded polystyrene concrete containing silica fume

K. Ganesh Babu*, D. Saradhi Babu

Structures and Materials Laboratory, Department of Ocean Engineering, Indian Institute of Technology Madras, Chennai 600 036, India

Received 17 January 2002; accepted 4 November 2002

Abstract

Lightweight concrete can be produced by replacing the normal aggregate with lightweight aggregate, either partially or fully, depending upon the requirements of density and strength. The present study covers the use of expanded polystyrene (EPS) beads as lightweight aggregate both in concretes and mortars containing silica fume as a supplementary cementitious material. The main aim of this project is to study the strength and the durability performance of EPS concretes. These mixes were designed by using the efficiency of silica fume at the different percentages. The resulting concretes were seen to have densities varying from 1500 to 2000 kg/m^3, with the corresponding strengths varying from 10 to 21 MPa. The rate of strength gain for these concretes shows that an increase in the percentage of silica fume increases the 7-day strength. This was observed to be about 75%, 85%, and 95% of the corresponding 28-day strength at the silica fume replacement levels of 3%, 5%, and 9%, respectively. The results of absorption, at 30 min and the final absorption, show that the EPS mixes made with sand have lower levels of absorption compared to the mixes containing normal aggregates. Further, the absorption values were seen to be decreasing with increasing cementitious content. The performance of these concretes, in terms of their chloride permeability and corrosion resistance, even at the minimal silica fume content level was observed to be very good.

Keywords: Expanded polystyrene; Silica fume; Strength; Water absorption; Chloride permeability; Corrosion

1. Introduction

The demand for lightweight concrete in many applications of modern constriction is increasing, owing to the advantage that lower density results in a significant benefit in terms of load-bearing elements of smaller cross sections and a corresponding reduction in the size of the foundation [1]. Lightweight aggregates are broadly classified in to two types—natural (pumice, diatomite, volcanic cinders, etc.) and artificial (perlite, expanded shale, clay, slate, sintered PFA, etc.). Expanded polystyrene (EPS) beads are a type of artificial ultra-lightweight (density of less than 300 kg/m^3), nonabsorbent aggregate [2,3]. It can be used to produce low-density concretes required for building applications like cladding panels, curtain walls, composite flooring systems, and load-bearing concrete blocks [4,5]. Also, it was reported that it can be used for other specialized applications like the sub-base material for pavement and railway track bed; as construction material for floating marine structures, sea beds, and sea fences; as an energy-absorbing material for the protection of buried military structures; and as fenders in offshore oil platforms [6–10]. By incorporating the EPS beads at different volume percentages in the concrete, mortar, or cement paste, a wide range of concrete densities can be achieved. The EPS aggregate replaces wholly or partly the normal aggregate in the case of concrete, or sand in the case of mortars.

Earlier researchers studied EPS mostly in mortar with Ordinary Portland Cement (OPC) as the binder. Also, to overcome its hydrophobic nature, bonding additives like water-emulsified epoxies and aqueous dispersions of polyvinyl propionate were added [11], or chemically treated EPS beads which are capable of preventing the segregation in the concrete mixes (commercially available as BST aggregate in Australia) were used [12]. Other investigators also reported that EPS tends to float and can result in a poor mix distribution and segregation, necessitating the use of admixtures [7,8]. Apart from this, most of the studies reported to

* Corresponding author. Tel.: +91-44-257-8623, +91-44-445-8623; fax: +91-44-235-0509.

E-mail address: kgbabu18@hotmail.com (K.G. Babu).

0008-8846/02/$ – see front matter © 2002 Published by Elsevier Science Ltd.
doi:10.1016/S0008-8846(02)01055-4

Table 1
Chemical composition of cement and silica fume

Chemical composition	Cement	Silica fume
Silica (SiO_2)	21.78	74.07
Alumina (Al_2O_3)	6.56	2.22
Ferric oxide (Fe_2O_3)	4.13	1.57
Calcium oxide (CaO)	60.12	2.95
Magnesium oxide (MgO)	2.08	1.27
Sodium oxide (Na_2O)	0.36	2.89
Potassium oxide (K_2O)	0.42	6.51
Sulphuric anhydride (SO_3)	2.16	0.95
Loss on ignition (LOI)	2.39	7.67

date were essentially on concretes of lower densities (below 1300 kg/m^3) resulting in strengths below 12 MPa.

The present study is an effort to develop structural lightweight concretes of 1440–1850 kg/m^3 with the corresponding strengths of about 17 MPa minimum [1]. Concretes containing silica fume as the supplementary cementitious material—with normal coarse aggregate and EPS, without adding any bonding additives—were investigated. Also, it is well understood that for concretes to qualify as structural materials, it is important that apart from the strength, durability and corrosion resistance parameters need a specific assessment. In view of this, the investigations included both parameters related to strength like compressive and split tensile strengths, and the durability parameters like water absorption, chloride permeability, corrosion rate, and accelerated corrosion cracking.

2. Mix proportions

2.1. Materials

Cement conforming to IS:12269 (C53 grade), which will also confirm to ASTM Type I, and silica fume were used as cementitious materials in the concrete mixes. The chemical characteristics of the cement and silica fume are given in Table 1. Series I and III contain sand finer than 2.36 mm, while Series II contains sand finer than 1.18 mm. The maximum size of the normal coarse aggregate (crushed blue granite) in Series I and II was 10 mm, while it was 16 mm for Mixes 8 and 10 and 20 mm for Mixes 9 and 11. In the present study, Mixes 10 and 11 were designed with the same total cementitious material and w/(c + s) ratio, as was reported earlier by Zhang and Gjorv [13] for lightweight concretes containing expanded clay-type aggregates. Two types of commercially available spherical EPS beads that are essentially single sized (Types A and B) were used. The grading shows that Type A has mostly 6.3-mm-size beads and Type B has mostly 4.75-mm-size beads. The bulk density and the specific gravity of these beads were 9.5 kg/m^3 and 0.014 for Type A and 20 kg/m^3 and 0.029 for Type B, respectively. A naphthalene-based superplasticizer was used to produce the mixes of flowable or highly flexible nature to suit the hand compaction adopted.

The design of EPS mixes with silica fume was based on the efficiency concept suggested earlier [14]. Three percentages of silica fume—3%, 5%, and 9% (by weight of the total cementitious materials), with the corresponding efficiency values of 7.5, 5.0, and 3.5—were used. The mixes were all designed as concretes considering the efficiency of silica fume. The reduction in the cement paste phase resulting from the high efficiency of silica fume was compensated to a certain degree by additional fines. The complete details of the concrete mixes are presented in Table 2.

2.2. Production of EPS concrete

Concrete was mixed in a planetary mixer of 100-l capacity. EPS beads were wetted initially with a part of

Table 2
Details of EPS concrete mixes containing silica fume

Sl number	Mix number	Cement (kg/m^3)	SF (s) (%)	Water (kg/m^3)	w/(c + s) ratio	Total aggregates (kg/m^3)	Sand[a] (kg/m^3)	Normal aggregates[b] (kg/m^3)	CA as EPS[c]		% Volume of EPS	SP % of TCM	Flow (mm)
									Type A (kg/m^3)	Type B (kg/m^3)			
Series I	1	350	3	158	0.440	1752	481	325	725	221	36.4	0.25	47
	2	362	3	164	0.440	1724	488	481	579	176	29.0	0.25	48
	3	375	3	170	0.440	1691	497	648	420	126	21.0	0.25	47
	4	335	3	152	0.440	1786	779	–	894	113	34.4	0.50	48
Series II	5	399	5	185	0.440	1606	498	530	–	578	22.2	0.5	52
	6	399	5	185	0.440	1606	1028	–	–	578	22.2	0.5	55
	7	399	5	185	0.440	1606	743	–	–	863	33.2	0.5	49
Series III	8	399	5	185	0.440	1606	337	515	321	433	28.7	0.25	51
	9	399	5	185	0.440	1606	337	515	321	433	28.7	0.5	53
	10	605	9	185	0.278	1454	305	466	291	392	26.3	0.5	58
	11	605	9	185	0.278	1454	305	466	291	392	26.0	0.75	55

CA—normal coarse aggregate; SF—silica fume.

[a] The size of sand used in Series II was 1 mm, downgraded; and in Series I and III, the sizes were 2.36 mm, downgraded.

[b] A 10-mm downgraded aggregate was used in Series I and II, 16 mm downgraded in Mixes 8 and 10, and 20 mm downgraded in Mixes 9 and 11.

[c] The weight of CA is converted to an equivalent volume of EPS (the bulk density of CA, EPS Type A, and Type B were 1600, 9.5, and 20 kg/m^3 respectively).

the mixing water and superplasticizer before adding the remaining materials. Mixing was continued until a uniform and flowing mixture was obtained. The fresh concrete densities and flow values were measured immediately after the mixing. The flow values varied between 47 and 58 cm and facilitated hand compaction. The specimens were cured under wet gunny bags initially and, after demolding, were stored in water.

3. Experimental investigations

3.1. Specimens and curing conditions

Standard test specimens of different sizes were chosen for investigating the various parameters. Cubes of 100 mm size were used for studying the compressive strengths at 1, 3, 7, 28, and 90 days and also for the absorption tests at 90 days. Split tensile strength test was conducted on 100 mm diameter × 200 mm cylinders at 28 days. Cylinders of 50 mm thickness and 100 mm diameter were used for the chloride permeability studies at 90 days. Cylinders of 100 mm diameter × 200 mm—with an 8-mm-diameter, hot-rolled, deformed steel bar of 100 mm of exposed length embedded in the middle—were used to study the corrosion rate and accelerated corrosion cracking. These specimens alone were cured in seawater until testing (90 days) after 3 days of normal water curing.

3.2. Test program

The flow values of the fresh concrete mixes were measured according to ASTM C 124-1973. Compressive strength test was carried out in a testing machine of 2000 kN capacity at a loading rate of 2.5 kN/s. The split tensile strength test was conducted on cylinders at 28 days as per ASTM C 496-89. The absorption test was carried out as per ASTM C 642-82. Saturated surface dry cubes were kept in a hot air oven at 60 °C (although ASTM suggests a temperature range of 100–110 °C) until a constant weight was attained. This is because at this temperature range of 100–110 °C, the EPS beads initially shrink and finally evaporate. These are then immersed in water and the weight gain is measured at regular intervals until a constant weight is reached. The absorption at 30 min and the final absorption (at a point when the difference between two consecutive weights at 12-h interval was almost negligible) were reported to assess the concrete quality.

The studies for the durability requirements were undertaken only on the concretes of Series I, as these contained the least amount of silica fume that improved the performance significantly (highest efficiency and a correspondingly lower cementitious materials content) and presented the lowest durability that can be expected. These were limited to chloride permeability, potential, corrosion rate, and accelerated corrosion studies.

The chloride permeability test was conducted to assess the concrete quality as per ASTM C 1202-94. A potential difference of 60 V DC was maintained across the specimen. One of the surfaces was immersed in a sodium chloride (NaCl) solution and the other in a sodium hydroxide (NaOH) solution. The total charge passing in 6 h was measured, indicating the resistance of the specimen to chloride ion penetration.

Potentiodynamic polarization technique was adopted to measure the corrosion rate of the 8-mm-diameter bars in the cylinder specimens, by using a scanning potentiostat (EG and G PAR-Model 362) and an X–log X, Y recorder. A potential of 250 mV was applied on either side of the open circuit potential (OCP), and the corrosion current (I_{corr}) was taken at 100 mV from the potentiodynamic plot. The corrosion rate was calculated from I_{corr} by using Faraday's equation.

Accelerated corrosion cracking study was performed on the same cylinder specimens containing a central 8-mm-diameter bar. The test was conducted in a 3% NaCl solution by impressing a current of 6 V for a period of 8 days. This part of the test was performed in accordance with the method proposed by the Florida Department of Transportation [15] and the average daily resistance was calculated. Later, to accelerate the corrosion process, a current of 60 V was applied for a period of 10 days or until a crack occurred. The current passing was measured at regular intervals to evaluate the charge to cracking.

4. Results and discussions

A comprehensive summary of the different strengths and absorption characteristics of all the concretes is presented in Table 3. The results of the corrosion-related parameters investigated for Series I, as already proposed, are given in Table 4.

4.1. Fresh concrete

The workability of the concrete in terms of the flow measurements was reported in Table 2. Flow values of the all the mixes were in the range of 47–58 cm. These flow values correspond to a slump of about 50–70 mm in most cases. The mixes having the higher percentage silica fume show higher flow values. All the concretes were flexible and easy to work with, and could be easily compacted using just hand compaction and could also be easily finished. The problems associated with the segregation and finishability of the mixes containing coarse beads as reported earlier [7] were totally solved by ensuring that a minimum amount of cementitious material was always present. The silica fume and the superplasticizer were essentially added to help solve the problems associated with the hydrophobic nature of the EPS beads and to improve the cohesiveness of the mix.

Table 3
Strength and absorption of EPS concrete mixes

Sl number	Mix number	Fresh concrete density (kg/m^3)	Compressive strength (MPa)					Split tensile strength (MPa)	Absorption (%)	
			1 day	3 days	7 days	28 days	90 days		30 min	Final
Series I	1	1552	4.2	6.6	7.6	10.2	10.6	1.53	0.695	5.424
	2	1698	5.8	7.2	11.2	15.0	14.0	2.04	0.903	5.355
	3	1979	10.2	12.8	14.0	21.4	21.2	2.16	1.049	4.882
	4	1503	4.4	6.8	8.4	10.2	12.2	2.10	0.741	4.596
Series II	5	1856	5.2	10.6	15.2	19.8	19.1	2.23	1.306	3.520
	6	1748	5.0	10.4	17.6	18.5	18.6	2.20	1.244	3.140
	7	1546	4.0	9.2	12.4	15.0	14.9	2.15	0.730	2.570
Series III	8	1762	6.6	10.2	11.6	12.0	11.2	1.83	1.350	3.630
	9	1771	4.6	9.8	14.2	17	17.2	2.02	1.250	3.150
	10	1793	9.8	13.4	15.6	16.2	16.5	2.22	1.270	2.540
	11	1873	9.8	16.4	19.8	20.8	21.2	2.32	1.000	2.340

4.2. Compressive strength

4.2.1. Effect of age

The variation of the compressive strength with age shows a continuous increase in almost all the mixes. The rate of strength development was greater initially and decreased as the age increased. The rate of strength gain at 7, 28, and 90 days is presented in Fig. 1. A comparison of strengths at 7 days reveals that concretes with 3% silica fume developed almost 75% of its 28-day strength, while that with 5% and 9% silica fume developed almost 85% and 95% of the corresponding 28-day strength. There was no appreciable strength improvement at 90 days. From this, it is clear that the rate of strength gain was increasing with an increasing percentage of silica fume.

4.2.2. Effect of density and EPS volume

The density of the concrete was controlled by varying the EPS volume in the mix. The variation of compressive strength with the plastic density of concrete (and percent volume of EPS) was presented in Fig. 2. The strength of EPS concretes appears to increase linearly with an increase in concrete density, or with a decrease in the EPS volume.

4.2.3. Effect of EPS bead size

The strength of EPS concrete increased with a decrease in the EPS bead size for the same mix proportions. This is clear from the results of the concretes of Series II made with only Type B (smaller EPS beads), which showed higher strength values, than the mixes made with the combination of Type A and Type B beads for the same concrete densities.

4.2.4. Effect of normal aggregate size

Comparing the strength results of Mixes 8 and 10 containing 16-mm, downgraded, normal coarse aggregate with those of Mixes 9 and 11 containing 20-mm, downgraded, normal coarse aggregate (Fig. 3), it is clear that the compressive strength increased with increasing aggregate size. The percentage increase in strength with size was also observed to be higher in the lean mixes compared to the rich mixes.

4.2.5. Effect of sand

Mixes 1 and 5 contain both sand and coarse aggregate while corresponding Mixes 4 and 6 contain only sand as the aggregate (mortar). The mix proportions of the two mix sets (Mixes 1 and 4, and Mixes 5 and 6) are also nearly the same. A comparison of the strength results of these two sets of mixes having comparable densities clearly shows that the effect of sand is negligible, both in terms of the strength gain rate as well as the strength at 90 days. However, it was observed that the mixes containing coarse aggregates always show a slight increase in density (about 50–100 kg/m^3).

4.2.6. Effect of lightweight aggregate strength

The strength of concrete is mainly influenced by the strength of the aggregate. The development of high-strength concretes is possible only when the aggregates have enough strength. Presently, Mixes 10 and 11 were designed with the same total cementitious material and w/(c + s) ratio as were reported earlier by Zhang and Gjorv [13]. They reported a 28-day compressive strength of 102.4 MPa for these concretes made with expanded clay aggregate. However, the 28-day strength for Mixes 10 and 11 containing EPS were only 16.2 and 20.8 MPa, respectively, in the present study.

Table 4
Corrosion studies on EPS concretes (Series I)

Sl number	Charge (C)	90-day OCP (− mV)	Corrosion rate at 100 mV (mpy)	ACC studies	
				ADR (Ω)	Total charge to cracking (C)
Mix 1	676.74	330	0.502	5.40	17,942
Mix 2	496.37	300	0.390	5.60	20,974
Mix 3	460.71	670	0.451	5.30	12,669
Mix 4	372.51	305	0.364	4.10	13,176

ACC—accelerated corrosion cracking; ADR—average daily resistance.

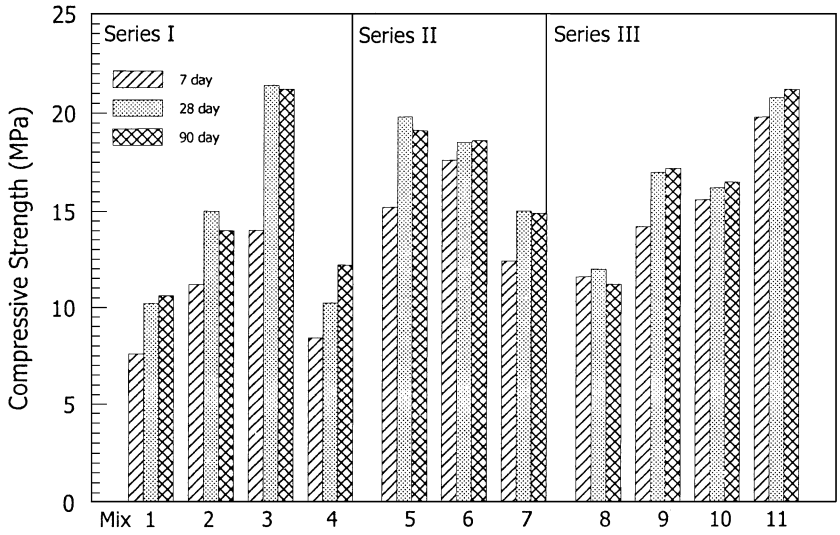

Fig. 1. Variation of compressive strength with age.

This wide variation of strength is mainly due to the difference in strength of the aggregates, as EPS aggregates have almost zero strength.

Moreover, the failure mode of the concrete specimens containing EPS aggregates under compressive loading did not exhibit the typical brittle failure normally associated with the conventional aggregate concrete. The failure observed was to be more gradual (more compressible), and the specimens were capable of retaining the load after failure without full disintegration. A similar type of failure was also reported earlier for plastic shredded aggregate concretes [16]. This clearly shows the high energy absorption capacity of these concretes that was suggested earlier [5,9].

4.3. Split tensile strength

The variation of tensile strength with the compressive strength is given in Fig. 4. From this, it can be seen that the tensile strength increased with an increase in compressive strength. The splitting failure mode of the concrete specimens containing EPS aggregates also did not exhibit the typical brittle failure normally observed in conventional concrete as in compressive strength. The failure observed

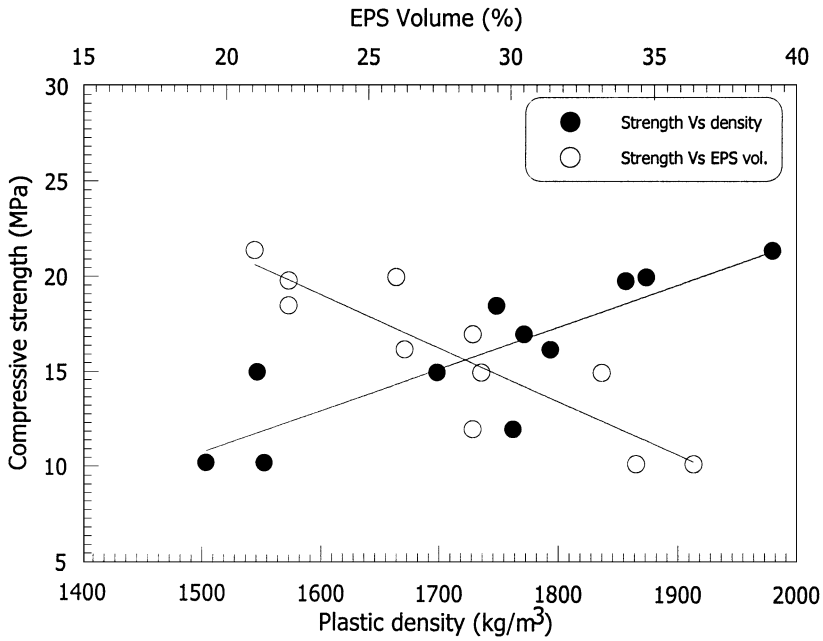

Fig. 2. Variation of strength with density and EPS volume.

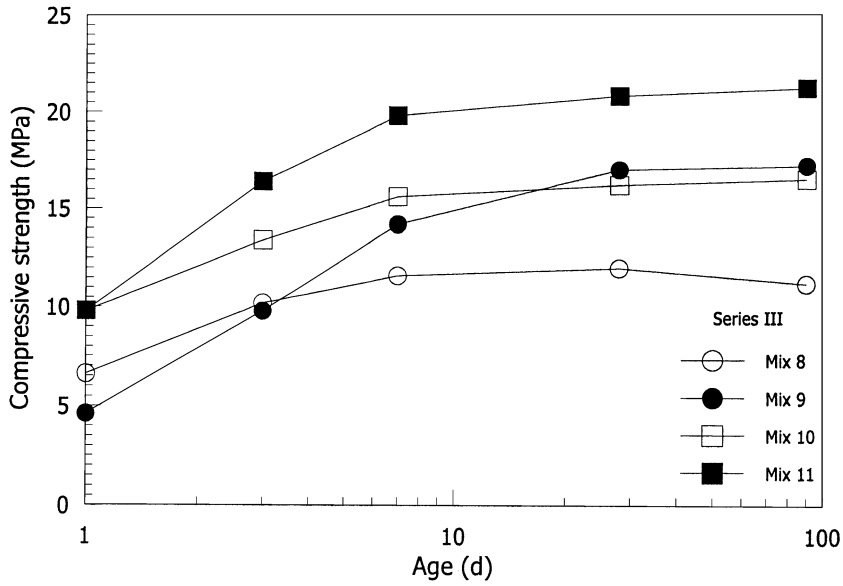

Fig. 3. Variation of compressive strength with age (Series III).

was more gradual (compressible) and the specimens did not separate in two, as was earlier reported for plastic shredded aggregate concretes [16].

4.4. Absorption

The durability of concrete primarily depends upon its permeability, which defines the resistance to the ingress of aggressive ions. The absorption characteristics indirectly represent the porosity, through an understanding of the permeable pore volume and its connectivity. A limit on the initial (30 min) absorption for assessing the concrete quality was defined by CEB earlier [17]. The initial absorption at 30 min, as well as the final (total) absorption, were shown in Fig. 5. As per the assessment criteria given by CEB, all the mixes in the present study showed a low absorption rating (<3% absorption), indicating a "good" concrete quality. Also, mixes with higher EPS percentages showed lower absorption values at the initial stage compared to the lower EPS percentage mixes. The total absorption values of EPS concretes, ranging from about 3% to 6%, decreased as the silica fume percentage increased. In comparison, Kluge et al. [18] reported the absorption values in the range of 8–25% by weight for concretes made with

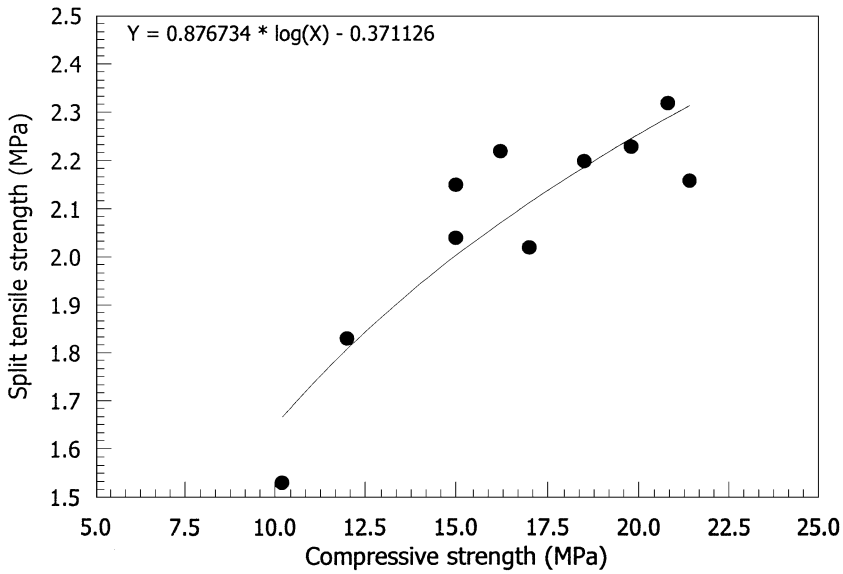

Fig. 4. Variation of split tensile strength with compressive strength.

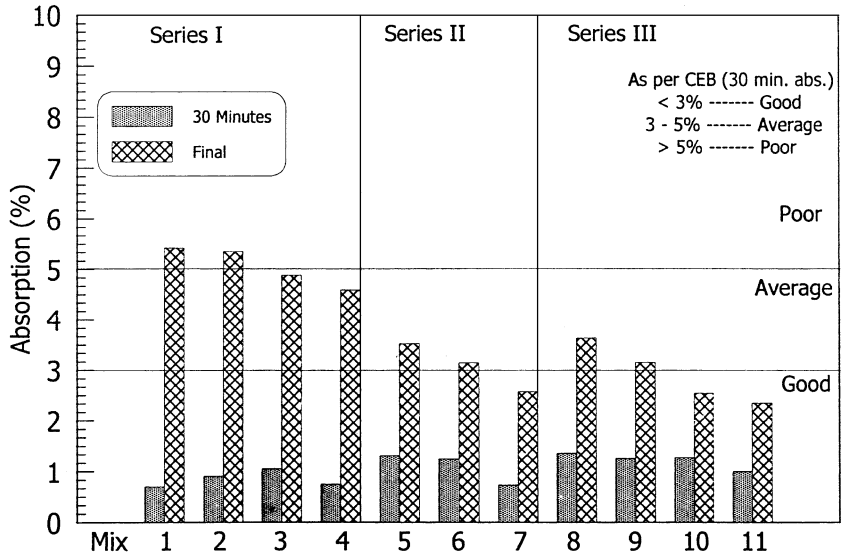

Fig. 5. Variation of the 30-min and the final absorption values.

artificial aggregates of even much higher crushing strength (processed lightweight aggregates like sintered fly ash, pumice, expanded shale, expanded slate, and expanded clay). This comparison was made only for concretes with similar densities and cement contents as in the present study. This could be attributed to the effect of silica fume and the advantage of the nonabsorbent nature of the EPS aggregate.

4.5. Chloride permeability

The resistance to chloride ion penetration is an important aspect that needs a better definition in structural materials. It is generally accepted that mineral admixtures significantly improve this through the chloride binding and pore filling effects. The pore filling effect is expected to be the factor that helps in the case of silica fume. The charge passing through these concretes ranged from 400 to 700 C, which is considered to be a very low chloride permeability. Also the concrete made with sand showed lower chloride permeability compared to the normal aggregate mixes. The results are similar to that observed for the high-strength concretes made with expanded clay aggregates reported earlier [19]. It was observed that the charge passing in these high-strength concretes containing silica fume also varied from 200 to 700 C, which compares well with the present investigation at the corresponding w/(c + s) ratios.

4.6. Potentials and corrosion rate

The potentials and the corrosion rates of the EPS concretes were not reported hitherto in literature. The OCPs and corrosion rates were measured at the age of 90 days. The potentials indicate that the steels are still in an active state (above −270 mV wrt SCE). The corrosion current (I_{corr}) of the embedded steel bar in EPS concretes was assessed using the potentiodynamic polarization plots. The corrosion rates of all the EPS concretes showed values around 0.4–0.5 mpy, which is significantly lower than that for the normal concretes.

4.7. Accelerated corrosion cracking

Corrosion is a long-term process and an exact evaluation of the corrosion resistance capability of the concrete composites is always intangible. Accelerated methods suggest the relative corrosion capability in a reasonably short period. The results of the accelerated corrosion cracking studies are presented in Table 4. The average daily resistance of these concretes was observed to be in the range of 2 kΩ. The EPS concretes also show a resistance to cracking similar to that of the normal concretes. This shows that the corrosion resistance of these low-strength lightweight concretes (12–20 MPa) is similar to that of the high-strength concrete, which can be achieved with the normal aggregate at the corresponding silica fume content and water cementitious materials ratio. These observations indicate that the corrosion properties mostly depend on the matrix composition and are not so much influenced by the aggregate properties.

5. Conclusions

All the EPS concretes without any special bonding agents show good workability and could be easily compacted and finished. The flow values increased with an increase in silica fume percentage.

The rate of strength development of the concretes increased with increasing percentage of silica fume. The strength of EPS concretes was found to be directly propor-

tional to the concrete density. The strength of EPS concrete marginally increased as the bead size decreased, and increased as the normal coarse aggregate size increased. This increase in strength was more in leaner mixes compared to the richer mixes.

The split tensile strength increased with an increase in the compressive strength. The compressive and splitting failures of the concrete specimens containing EPS aggregates show a large compressibility of the material and did not exhibit the typical brittle failure normally associated with the conventional concrete.

All the EPS concretes show a low absorption rating (below 3% at 30 min) indicating concrete of "good" quality. Also the total absorption values decreased with increasing silica fume percentage.

As per the assessment criteria, all the EPS concretes containing silica fume showed a low chloride permeability of <1000 C. These concretes also exhibited much lower corrosion rates compared to the normal concrete. The average daily resistance and the charge to cracking were similar to that of normal concrete, which shows that the corrosion properties mostly depend on the matrix composition and are not so much influenced by the aggregate properties.

References

[1] ACI Committee 213 R-87, Guide for Structural Lightweight Aggregate Concrete, ACI Manual of Concrete Practice, Part 1, American Concrete Institute, Farmington Hills, 1987.
[2] A. Short, W. Kinniburgh, Lightweight Concrete, 3rd ed., Applied Science Publishers, London, 1978.
[3] V. Sussman, Lightweight plastic aggregate concrete, ACI J. (1975, July) 321–323.
[4] D.J. Cook, in: R.N. Swamy (Ed.), Expanded Polystyrene Concrete, Concrete Technology and Design: (1). New Concrete Materials, Surrey University Press, London, 1983, pp. 41–69.
[5] A. Godwin, Versatile concrete blocks for the third world, Indian Concr. J. (1982, September) 240–241.
[6] A.N. Hanna, Properties of expanded polystyrene concrete and applications for pavement sub-bases, Res. Develop. Bull.-Portland Cem. Assoc. (Rd 055.01P).
[7] C. Bagon, S. Frondistou-Yannas, Marine floating concrete made with polystyrene expanded beads, Mag. Concr. Res. 28 (1976) 225–229.
[8] S.H. Perry, P.H. Bischaff, K. Yamura, Mix details and material behaviour of polystyrene aggregate concrete, Mag. Concr. Res. 43 (1991) 71–76.
[9] G.C. Hoff, New applications for low density concretes, Lightweight Concrete, ACI SP, vol. 29, American Concrete Institute, Detroit, 1971, pp. 181–220.
[10] P.H. Bischoff, K. Yamura, S.H. Perry, Polystyrene aggregate concrete subjected to hard impact, Proc.-Inst. Civ. Eng. 2. Res. Theory 89 (1990) 225–239.
[11] D.J. Cook, Expanded polystyrene beads as lightweight aggregate for concrete, Precast Concr. 4 (1973) 691–693.
[12] R. Sri Ravindrarajah, A.J. Tuck, Properties of hardened concrete containing treated expanded polystyrene beads, Cem. Concr. Compos. 16 (1994) 273–277.
[13] M.H. Zhang, O.E. Gjorv, Mechanical properties of high strength lightweight concrete, ACI Mater. J. 88 (3) (1991) 240–247.
[14] K. Ganesh Babu, P.V. Surya Prakash, Efficiency of silica fume in concrete, Cem. Concr. Res. 25 (6) (1995) 1273–1283.
[15] R.P. Brown, R.J. Kesseler, An accelerated laboratory method for corrosion testing of reinforced concrete using impressed current, Research Report 206, Florida Department of Transportation, 1978.
[16] A.A. Al-Manaseer, T.R. Dalal, Concrete containing plastic aggregates, Concr. Int. (1997, August) 47–52.
[17] CEB-FIP, Diagnosis and assessment of concrete structures—"State of the Art Report", CEB Bull. 192 (1989) 83–85.
[18] R.W. Kluge, M.M. Sparks, E.C. Tuma, Lightweight aggregate concrete, ACI J. (1949, May) 625–642.
[19] M.H. Zhang, O.E. Gjorv, Permeability of high strength lightweight concrete, ACI Mater. J. 88 (2) (1991) 463–469.